GE

Form Approved
OMB No. 0704-0188

1. AGENCY USE ONLY (Leave blank)	2. REPORT DATE	3. REPORT TYPE AND DATES COVERED
	1994	1994

4. TITLE AND SUBTITLE
Surface Composition of a Series of Dimethylsiloxane Urea, Urethane Segmented Copolymers Studied by Electron Spectroscopy for Chemical Analysis

5. FUNDING NUMBERS

6. AUTHOR(S)
Xin Chen, Joseph A. Gardella, Jr., and Tai Ho

7. PERFORMING ORGANIZATION NAME(S) AND ADDRESS(ES)
Department of Chemistry, NSM Complex
State University of New York, University at Buffalo
Buffalo, NY 14260-3000

8. PERFORMING ORGANIZATION REPORT NUMBER
94-01

9. SPONSORING/MONITORING AGENCY NAME(S) AND ADDRESS(ES)
Department of the Navy, Office of Naval Research
800 North Quincy Street, Arlington, VA 22217-5660

10. SPONSORING/MONITORING AGENCY REPORT NUMBER

11. SUPPLEMENTARY NOTES

12a. DISTRIBUTION/AVAILABILITY STATEMENT
This document has been approved for public release and sale; its distribution is unlimited.

12b. DISTRIBUTION CODE

13. ABSTRACT (Maximum 200 words)
Surface composition of a series of segmented poly(siloxane urea urethane)'s have been determined by angle- and energy-dependent ESCA. The polymers are based on aminopropyl end-capped dimethylsiloxane oligomers, isophorone diisocyanate and 1,4-benzene dimethanol. Effects of segmental length and annealing on the surface composition were investigated. It was found that when the average molecular weight of the siloxane segments reaches 27K, the topmost surface region (within 18 Å of the free surface) of a film cast from tetrahydrofuran solution is nearly siloxane phase. To achieve a comparable degree of surface phase enrichment in films of copolymers with siloxane segmental molecular weight of 10K, annealing at 120°C for 15 minutes was required. Depth profiles based on these data showed that in as-cast films a siloxane deficient phase several nanometers thick occurs beneath the siloxane surface layer. Annealing increases the thickness of both surface phases.

14. SUBJECT TERMS

15. NUMBER OF PAGES
49

16. PRICE CODE

17. SECURITY CLASSIFICATION OF REPORT	18. SECURITY CLASSIFICATION OF THIS PAGE	19. SECURITY CLASSIFICATION OF ABSTRACT	20. LIMITATION OF ABSTRACT
Unclassified	Unclassified	Unclassified	UL

OFFICE OF NAVAL RESEARCH

GRANT N0001493310058

R&T Code 4132083
Kenneth J. Wynne

Technical Report No. 94-01

Surface Composition of a Series of Dimethylsiloxane Urea, Urethane Segmented Copolymers Studied by Electron Spectroscopy for Chemical Analysis

by

Xin Chen, Joseph A. Gardella, Jr., and Tai Ho

Prepared for Publication

in

Macromolecules

State University of New York at Buffalo
Department of Chemistry
Buffalo, NY

March, 1994

Surface Composition of A Series of Dimethylsiloxane Urea, Urethane Segmented Copolymers Studied by Electron Spectroscopy for Chemical Analysis

Xin Chen, and Joseph A. Gardella, Jr.

Department of Chemistry,

State University of New York at Buffalo,

Buffalo, NY 14214

Tai Ho

Department of Chemistry, George Mason University

Fairfax, Virginia 22030-4444

Kenneth J. Wynne

Chemistry Division, Office of Naval Research

Arlington, VA 22217-5000 and

Materials Chemistry Branch, Naval Research Laboratory

Washington, D.C. 20375-5320

submitted to Macromolecules

March, 1994

Abstract

Surface composition of a series of segmented poly(siloxane urea urethane)'s have been determined by angle- and energy-dependent ESCA. The polymers are based on aminopropyl end-capped dimethylsiloxane oligomers, isophorone diisocyanate and 1,4-benzene dimethanol. Effects of segmental length and annealing on the surface composition were investigated. It was found that when the average molecular weight of the siloxane segments reaches 27K, the topmost surface region (within 18 Å of the free surface) of a film cast from tetrahydrofuran solution is nearly siloxane phase. To achieve a comparable degree of surface phase enrichment in films of copolymers with siloxane segmental molecular weight of 10K, annealing at 120°C for 15 minutes was required. Depth profiles based on these data showed that in as-cast films a siloxane deficient phase several nanometers thick occurs beneath the siloxane surface layer. Annealing increases the thickness of both surface phases.

Introduction

We are interested in multicomponent polymers and the thermodynamic and kinetic effects which influence the nature of the polymer surfaces. Our goal is to discern the compositional and morphological features relevant to the formation of minimally adhesive surfaces which inhibit the settlement of marine organisms.[1]

We have previously reported the synthesis and characterization of polyurethanes based on a series of fluorinated diols and hexamethylene diisocyanate.[2] Analysis of contact angle and angle resolved electron spectroscopy data[3] revealed that surface composition and properties were identical to the bulk. To achieve surface phase separation of the low surface energy polymer component, longer chain length diols containing low surface energy segments were sought. In a continuation of this work and with the dual criteria of creating surfaces with low surface energy and low T_g to minimize mechanical locking of a prospective adherent, we have prepared and characterized a series of segmented copolymers based on aminopropyl end-capped dimethylsiloxane oligomers and isophorone diisocyanate (IPDI) with 1,4-benzene dimethanol (BDM) as the chain extender, and investigated the effects of chain extenders on material properties.[4]

Surface composition and morphology of block copolymers containing poly(dimethylsiloxane) (PDMS) segments have been previously studied using angle-dependent electron spectroscopy for chemical analysis (ESCA), cross-sectional transmission electron microscopy (TEM) and attenuated total reflectance Fourier transform infrared spectroscopy (ATRFTIR). The scope of materials investigated includes PDMS-nylon-6,[5] poly(α-methylstyrene)-PDMS,[6] (bisphenol A polycarbonate)-PDMS,[7,8] and polystyrene-PDMS[9,10] of various block architectures and overall compositions. Enrichment of PDMS segments in surface region was detected in each case due to the lower surface energy of PDMS component in these block copolymers.

This work builds on the observation that surface composition of multicomponent polymers depends on not only their structure, but also sample history. It was shown that surface composition of solution cast films of block copolymers can be changed by either using selective solvents[4,11] or by annealing.[4,5,7,12]

We are interested in the region within 100 Å of the air-polymer interface, and ESCA has been established as an effective tool to probe this region. However, photoelectron intensities detected by ESCA are convoluted signals, i.e. all atoms within the path of the probing X-ray contribute to the signal but the contribution of each decreases exponentially with the distance from the free surface.[13] The convoluted nature of the signal distorts depth profiles for samples with compositional gradients. To recover the

depth profiles for such samples, a de-convolution procedure must be applied to the ESCA data.

Several research groups have addressed this problem of de-convolution. The methods developed generally involve introducing additional constraints to the equations describing the convoluted signals. These equations can be solved numerically,[14] by inverse Laplace transform,[15,16] or by the method of regularization.[17,18,19] In this paper we show that, with the constraints generally adopted in the de-convolution process, depth profiles of the individual segments in a segmented copolymer can be reconstructed from ESCA data by numerical methods. Ratner and co-workers have solved a similar problem by the method of regularization.[18]

Experimental

A series of segmented copolymers based on aminopropyl end-capped dimethylsiloxane oligomers (PDMS) and isophorone diisocyanate (IPDI) with 1,4-benzene dimethanol (BDM) as the chain extender were prepared with a two-step polymerization. First, reaction between IPDI and BDM was carried out in bulk at elevated temperature without catalyst. In the second stage, the reaction between PDMS oligomers and diisocyanate intermediates was carried out in tetrahydrofuran (THF) solution at room temperature. Details of the synthetic procedure have been described in a separate publication.[10] The structure of these polymers is shown

in Figure 1 and molecular weight data listed in Table I. Nomenclature for the copolymers is as follows, illustrated for PDMS27K-IP-B2, where PDMS27K identifies the average molecular weight of the soft segment, IP the diisocyanate (IPDI), and B the chain extender (BDM), and 2 is the molar ratio of the chain extender to the siloxane oligomer. The copolymers are also designated as PDMS-PU copolymers.

Before the preparation of the films, the copolymers were soaked in an excess amount of hexane for one day, to remove unreacted siloxane oligomers. The copolymers were then removed from the solvent and dried in a vacuum oven at 50°C overnight. The dried copolymers were dissolved in THF to make 0.5-1 % solutions. The polymer solutions were cast into clean aluminum weighing pans, and then allowed to dry in air. The films were further dried in a vacuum oven at ambient temperature for over 2 days to obtain "as-cast" films. Using the solution concentration and volume, the thickness of the films was estimated at ~50 μm. Film annealing was accomplished by heating in a vacuum oven at 120 °C for 15 minutes (short annealing) or 2 hours (long annealing). The annealing temperature was chosen to be about 25° above the highest transition temperature (about 100°C) detected by dynamic mechanical analysis.[10] No other treatment was applied to the polymer films before analysis.

Angle-dependent ESCA experiments were performed on a Perkin-Elmer Physical Electronic Model 5300 ESCA with a hemispherical analyzer and a single channel detector. The ESCA spectrometer was equipped with both Mg Kα and Ti Kα X-ray sources, and each was operated at 300 Watts (15 KV and 20 mA). The base pressure was maintained at lower than 10^{-8} torr. A pass energy of 35.75 eV was chosen for all high resolution angle dependent acquisitions. Four take-off angles, at 10°, 15°, 30°, and 90°, were used with the Mg Kα X-ray source, while a single take-off angle at 90° was used for Ti X-ray ESCA acquisitions. The take-off angle is defined such that the direction normal to the surface of the material is 90°.

The number of measurements using Ti Kα X-ray source was reduced to prevent radiation degradation of samples, since the kinetic energy of Ti Kα X-ray (4510.9 eV) is much higher than that of Mg Kα X-ray (1253.6 eV) and the acquisition time is longer to compensate for a lower Ti X-ray intensity.[20] Sampling depth, d_s, was calculated from equation $d_s = 3 \lambda \sin \theta$, where λ is the escape depth of the photoelectrons and θ the take off angle. The escape depth can be estimated from empirical equations that correlate this quantity with the kinetic energy of the photoelectrons.[5,21]

Thin films of nylon-6 (atomic ratio of N to C is 1/6) and poly(γ-benzyl glutamate) (atomic ratio of N to C is 1/12) were used to calibrate the atomic sensitivity factor ratio of nitrogen to

carbon under the same ESCA experimental conditions applied to the copolymer samples.

For quantifying ESCA signals in carbon 1s, nitrogen 1s, silicon 2p, and oxygen 1s regions spectra were recorded at high resolution conditions. ESCA peak areas were measured by a Perkin-Elmer 7500 computer with the PHI ESCA version 2.0 software. An average of three independent runs was taken for all ESCA measurements.

Calculations

For convenience, the PDMS-PU segmented copolymer chains are divided into soft and hard segments. A soft segment is an oligomeric siloxane with the two $-NH_2$ end group moieties excluded, since the $-NH_2$ groups become part of the urea groups after polymerization. A hard segment consists of the two urea groups from reactions between IPDI and the siloxane oligomers and the moieties of IPDI and BDM. The average number of IPDI and BDM moieties in a given hard segment depends on the reaction stoichiometry. For example, the hard segment of sample 5 (Table I) is composed of 2 $-NH_2$, 3 IPDI, and 2 BDM groups. The soft segment for this sample is a siloxane oligomer of 30 repeat units (MW = 2400).

The relationship between the weight percentage of PDMS (X) and the ratio of nitrogen atoms to carbon atoms, N/C, measured by ESCA is expressed by Equations (1-6).

$$\frac{N}{C} = \frac{[(100-X)/(MW_{hard})] \quad (\#^{N}_{hard})}{[(100-X)/(MW_{hard})] \quad (\#^{C}_{hard}) + [X/MW_{soft}] \quad (\#^{C}_{soft})} \tag{1}$$

$$MW_{hard} = 222 \quad \#^{IPDI} + 138 \quad \#^{BDM} + 32 \tag{2}$$

$$MW_{soft} = 74 \quad n + 142 \tag{3}$$

$$\#^{N}_{hard} = 2 \quad \#^{IPDI} + 2 \tag{4}$$

$$\#^{C}_{hard} = 12 \quad \#^{IPDI} + 8 \quad \#^{BDM} \tag{5}$$

$$\#^{C}_{soft} = 2 \quad (n + 1) + 6 \tag{6}$$

Here, n is the number of repeat units in each siloxane oligomer, $\#^{IPDI}$ and $\#^{BDM}$ are the numbers of IPDI and BDM, respectively, in a hard segment. The numbers of carbon atoms in a hard segment and a soft segment are $\#^{C}_{hard}$ and $\#^{C}_{soft}$. Nitrogen atoms only exist in the hard segments and each hard segment contains $\#^{N}_{hard}$ nitrogen atoms. The molecular weight of a hard segment is MW_{hard} and the molecular weight of a soft segment is MW_{soft}. The conversion formulas from N/C ratio to X are listed in Table II.

The ratio of N/C, instead of Si/C, is chosen to calculate the PDMS surface concentrations because of the larger variation in nitrogen concentration at different sampling depths. This results in higher sensitivity in PDMS wt.% calculation. Concentrations were also calculated from Si/C ratios for a selected set of

samples. The resultant concentration data fell within error limits as equivalent to that calculated from N/C ratios.

Recovery of Depth Profile from ESCA Data

The intensities of the photoelectronic response from nitrogen and carbon atoms as functions of the take-off angle can be formulated in the derivative form. They are

$$dI_N(\theta) = F\alpha_N N_N(x)\ K\ e^{-x/(\lambda_N \sin\theta)}\ dx \qquad (7)$$

$$dI_C(\theta) = F\alpha_C N_C(x)\ K\ e^{-x/(\lambda_C \sin\theta)}\ dx \qquad (8)$$

where I is the detected intensity of photoelectrons from a given atom, subscripts N and C denote nitrogen and carbon, respectively, θ is the take-off angle, F is the X-ray flux, α is the cross section of photoionization in a given shell of a given atom for a given X-ray energy, N(x) the depth profile of the atomic density, x is the vertical distance from the free surface, K is a spectrometer factor, and λ is the escape depth of the electrons.[13]

If one further assumes F, K and α are independent of x, and define normalized intensity $I'(\theta)$ as $I(\theta)/(F\alpha K)$. By integration, equations 7 and 8 give

$$I_N'(\theta) = I_N(\theta)/(F\alpha_N K) = \int_0^\infty N_N(x)\, e^{-x/(\lambda_N \sin\theta)}\, dx \qquad (9)$$

$$I_C'(\theta) = I_C(\theta)/(F\alpha_C K) = \int_0^\infty N_C(x)\, e^{-x/(\lambda_C \sin\theta)}\, dx \qquad (10)$$

Normalized intensities for different atoms at a take off angle θ, usually reported as a ratio, such as I_N'/I_C', can be obtained from the ESCA spectrum.

Atomic Density Profiles

Surface atomic density profiles for nitrogen and carbon in the segmented copolymers were obtained with the following procedures. The polymer chains were first divided into soft and hard segments as described above. Number densities of carbon atoms in each type of segment were calculated to be from 25.8 to 28.7 mole/liter for the soft segments, 45.5 mole/liter for non-chain extended hard segments, and from 52.5 to 54.3 mole/liter for chain extended hard segments as shown in Table III. To calculate the atomic densities in the copolymer, it was assumed that changes in density throughout the film (< 5%) and the difference between weight fraction and volume fraction values(< 3%) are negligible. Thus, if v(x) is the depth profile of the hard segments, atomic depth profiles for carbon and nitrogen are

$$N_C(x) = \eta\, v + \sigma\, (1 - v) \qquad (11)$$

$$N_N(x) = \eta\, v\, \gamma \qquad (12)$$

where η and σ are, respectively, the carbon densities for the hard segment and the soft segment, and γ is the nitrogen to carbon ratio in the hard segment. Values of these coefficients for each polymer are listed in Table IV.

The depth profiles described by equations 11 and 12 are inserted into equations 9 and 10. The ratio of the detected intensities of photoelectrons from carbon and nitrogen, now designated as **R**, can be calculated and compared with experimental values.

Recovery of the Depth Profile

To facilitate the calculation, it was further assumed that photoelectrons from carbon and nitrogen atoms have the same escape depth λ. This enabled us to express the depth profile in terms of a normalized length *l*, which is defined as the distance from the free surface, x, divided by the electron escape depth, λ. Depth profiles of the volume fraction of the hard segment, v(x), were approximated by both discrete and continuous models.

The Discrete Model

In the discrete model, v(x) is approximated as the sum of nine step functions. Each step function staggers the previous one by a distance varying from 0.1 to 0.85 λ determined by trial and error. The integrations described by equations 9 and 10 were carried out numerically, each as the summation of a sequence of numerical values. The upper limit for the integration was 5 λ, and the increment was λ/100. By continually adjusting the heights of the constituent step functions, a depth profile was obtained that gives photo-electronic responses consistent with ESCA results for each copolymer.

The Continuous Model

In fitting the experimental data with the discrete model, it was revealed that v(x), instead of being monotonously increasing with x, has a maximum. This finding was used to guide the selection of a continuous function to describe v(x). We used a four-parameter compound Gaussian distribution model of the form

$$y(\lambda) = y_1 \, \mathrm{Exp}[-0.5 \, (\lambda - \lambda_1)^2/\sigma_1^2] \qquad \lambda \le \lambda_1$$

$$= 1 + (y_1 - 1) \, \mathrm{Exp}[-0.5 \, (\lambda - \lambda_1)^2/\sigma_2^2] \qquad \lambda > \lambda_1 \qquad (13)$$

where y: $v(\lambda)/\, v(\infty)$, $v(\infty)$ is the bulk value of v;

y_1: a parameter, y value at the maximum of the profile;

λ: distance from surface /escape depth;

λ_1: a parameter, location of the maximum of the profile;

σ_1: a parameter, which characterizes the shape of the profile to the left of the maximum;

σ_2: a parameter, which characterizes the shape of the profile to the right of the maximum.

Optimal values for the parameters were determined by minimizing the objective function ψ defined as

$$\psi = \left\{ 1/n \sum^{n} \left\{ [R_{calc}(y_1, \lambda_1, \sigma_1, \sigma_2, \theta_n) - R_{exp}(\theta_n)] / R_{exp}(\theta_n) \right\}^2 \right\}^{1/2} \qquad (14)$$

where n is the number of take-off angles. The optimization was achieved using the Gauss-Newton method.[22] The starting values for the optimization procedures were obtained by scanning the five-dimensional space. In the latter, a grid was imposed on the $(y_1, \lambda_1, \sigma_1, \sigma_2)$ space, ψ values at selected intersections were calculated, and the coordinates of the location where the minimum was found were used as the starting values.

Results and Discussion

Surface Composition of PDMS-PU Films by ESCA.

Structural Effects. The measured PDMS surface concentrations of the PDMS-PU segmented copolymer films cast from THF in air are summarized in Table V. The surface concentrations of PDMS in all samples are higher than the bulk values. PDMS surface phase separation can be attributed to the lower surface energy of PDMS segments at the polymer-air interface as compared with that of the polar hard segments.[23] ESCA results for the PDMS-PU segmented copolymers are angle dependent indicating a gradient in concentration of PDMS over the surface region.

The average soft and hard segmental lengths are found to have significant effects on the surface composition. Concentrations of PDMS in the surface region of the as-cast films of polymers PDMS1K-IP-B0, PDMS2.4K-IP-B0 and PDMS10K-IP-B0 are compared in Figure 2. There is no chain extender in the hard segments of these three copolymers, and the average molecular weights of the PDMS segments are 1, 2.4, and 10K. In this series, polymer PDMS10K-IP-B0 shows the highest PDMS surface concentration at every take-off angle.

Surface compositions of the as-cast films of three copolymers PDMS2.4K-IP-B2, PDMS10K-IP-B2 and PDMS27K-IP-B2 are compared in Figure 3. Each hard segment of these copolymers contains on

average two BDM moieties, and the average molecular weights for the soft segments are 2.4, 10, and 27K, respectively. Again, the sample with the highest average molecular weight for the soft segments has the highest PDMS surface concentration.

Figure 4 illustrates the change in PDMS surface concentration with increase in the length of hard segment. In this group of PDMS-PU samples, the average molecular weights for the soft segments are the same, but the average lengths for the hard segment are different. It appears that the surface concentration of PDMS decreases as the length of the hard segment increases. Comparison can also be made for samples with similar *bulk* PDMS concentrations. For such samples, the length ratios of PDMS segment to hard segment are similar. Copolymers PDMS1K-IP-B0 and PDMS10K-IP-B2 have similar bulk concentrations of PDMS (90.3% and 91.1%). Results for these two copolymers are compared in Figure 5. Copolymer PDMS10K-IP-B2, which has larger average segmental lengths, shows higher surface concentration of PDMS in three take-off angles, while difference between results from the fourth take-off angle is less than the experimental uncertainty. These data indicate that for copolymers with similar bulk compositions, the thickness of the phase separated regions at the surface is influenced by the length of the low surface energy soft block. To understand the significance of the two comparisons described above, proper consideration must be given to the fact that the composition of the hard segments changes with the length.

Therefore, in addition to phase separation due to favorable entropic effect of longer soft segments, of equal or greater importance is phase separation driven by enthalpic effect of stronger hydrogen bonding of larger hard blocks. These two effects may act in a synergistic fashion. This topic will be explored further in a later section.

The molecular weight distributions for the eight samples are very different, with polydispersities ranging from 1.3 to 2.8. It is not clear from our study what effect polydispersity may have on surface properties.

Annealing Effects. The surface compositions of PDMS-PU copolymer samples after a short annealing as measured by ESCA are summarized in Table VI, and corresponding data for samples after a long annealing are listed in Table VII.[24]

For samples with the shortest PDMS segments (MW_{soft} = 1000), annealing does not have any detectable effect on the surface concentration of PDMS. For samples with PDMS segments of moderate length (MW_{soft} = 2.4K), the only increase in PDMS surface concentration was observed in the sample with the longest hard segments. An annealing of fifteen minutes at 120 °C was sufficient to cause the observed change. If the PDMS segments are long (MW_{soft} = 10K), significant changes in the PDMS surface concentrations are observed regardless the composition of the

hard segment. For example, the concentration of PDMS in the as-cast films of PDMS10K-IP-B0 and PDMS10K-IP-B2 measured at the lowest take off angle are 98.9 and 97.7 %, respectively, after annealing, the corresponding values are 99.9 and 99.4 %. The annealing effect on PDMS10K-IP-B2 sample is demonstrated in Figure 6. The dominance of PDMS segments in the surface region is even more pronounced in copolymer PDMS27K-IP-B2. No hard segments were detected in measurements taken at the lowest take-off angle, and the topmost surface regions of both as-cast and annealed films contain only PDMS component.

The maximum sampling depth in ESCA measurements using a Ti anode is estimated to be 210 Å, which is about twice the maximum sampling depth attainable with a Mg anode. By using a Ti anode, the composition over a larger span of polymer surface can be evaluated. In Table VII surface compositions of the films after a long annealing are listed including results from a sampling depth at 210 Å. A continuous decrease in the concentration of PDMS in the surface region was observed.

Segmental Concentration Depth Profile. Depth profiles for the hard segment in each copolymer have been recovered, and the profiles reveal some features that are not obvious in the ESCA data. In the following, the depth profile for the hard segment in copolymer PDMS2.4K-IP-B2 is used as a representative result to illustrate these features. In Figure 7, curve A represents the

profile suggested by the continuous model, curve B the profile suggested by the discrete model, and the filled points data measured with ESCA. The curves were generated based on experimental data and parameters listed in Table VIII, Table IX, and Table X, the keys to read these tables are contained in Table XI. Both models indicate a maximum in the profile in contrast to a monotonously increasing profile suggested by the ESCA data. The ESCA data also give a lower hard segment content in the surface region than the models. These discrepancies underline the fact that for polymers with partially or completely phase separated surface regions, the convoluted nature of the photoelectron intensity signals prevents a direct measurement of concentration depth profiles. Profiles suggested by both models, when inserted into the convolution equations, lead to photoelectron intensity ratios in very good agreement with experimental data as shown in Table VIII. Effects of annealing on depth profiles are shown in Figure 8 (based on the discrete model), and in Figure 9 (based on the continuous model). Both models reveal increases in the thickness of PDMS and hard-block enriched phases after annealing. The thickness of the topmost PDMS layer with less than 5% hard segment content increases from zero to 0.2 λ (about 0.7 nm). The thickness of the layer enriched with hard segments, which is responsible for the maximum in the profile, doubles from ~λ to ~2λ. These observations again illustrate the positive effects of annealing in enhancing the surface concentration of PDMS.

Effects of Structure and Molecular Weight on the Distribution of the Hard Segment. In addition to the difference in surface energies, which is the underlying driving force for the enrichment of PDMS segments at the surface, there are two additional factors that contribute to the observed surface phase separation. Long soft segments amplify entropically driven phase separation, and increased hydrogen bonding in hard segments augments the enthalpic driving force for phase separation. The interplay of these factors under different situations is discussed below.

We define $v_N(x)$ as

$$v_N(x) = \{v(x)/[1-v(x)]\} / \{v(\infty)/[1-v(\infty)]\} \qquad (15)$$

Equation 15 represents the normalization of the volume fraction of the hard segment at the surface region, $v(x)$, with respect to the bulk value, $v(\infty)$. The quantity $v_N(x)$ can also be visualized in the following way. Suppose a unit volume of soft segments with the entrapped hard segments moves from the bulk (location ∞) to the surface (location x), and during the movement the hard segments gradually drop out this volume due to the progress of phase separation, then $v_N(x)$ represents the fraction of the initial hard segments remaining at the end of the movement. Using this measurement, materials can be compared based on their "effectiveness" in separating the soft and the hard segments.

In Figure 10, v_N depth profiles for copolymers PDMS10K-IP-B0 (A, C) and PDMS10K-IP-B2 (B,D) are shown. The curves are for films as-cast and after an annealing at 120°C for 15 minutes. These curves are similar to those for PDMS2.4K-IP-B2 described earlier. There is a hard segment enriched region beneath the hard segment deficient surface layer, and annealing increases the thickness of both layers. In this section we will focus on the lower left corner of Figure 10 representing the region less than one λ (ca. 3.4 nm) from the surface. That portion is enlarged and roplotted in Figure 11. The two solid curves (A, B), representing concentration profiles in the as-cast films, indicate that the incorporation of chain extender promotes surface phase separation at ambient temperature presumably due to the increased interactions among the hard segments. This advantage is lost in annealing as both after-annealing profiles (dashed curves) are similar and shift to lower hard segment concentrations. Since the soft segments are the same and relatively large compared to the hard segments, the occurrence of the similar near-surface profiles after short annealing is driven by enthalpy. Thus, the rate of disadvantaged phase separation for PDMS10K-IP-B0 catches up to that of PDMS10K-IP-B2, as an increase in temperature enhances the higher-energy barrier phase separation process for PDMS10K-IP-B0.

In Figure 12, v_N profiles for copolymers PDMS2.4K-IP-B2, PDMS10K-IP-B2, and PDMS27K-IP-B2 are plotted. Cast at ambient

temperature, the hard segment concentration in the surface region decreases with increase in the average molecular weight of the soft segments. After annealing, the curves shift to lower hard segment concentrations while the relative positions to one another are maintained. The inverse correlation between surface hard segment concentration and bulk soft segment molecular weight as well as the insensitivity of the shape of the curve to temperature points to entropic origins for the observed differences.

Conclusions

We have investigated the effects of segmental length and annealing on the surface composition of films of segmented poly(dimethylsiloxane urea urethane)'s. The films were cast from solutions in THF, a mutual solvent for the hard and soft segments. In general, surface concentration of PDMS increases with the length of that segment. As PDMS segmental molecular weight reaches 27,000, ESCA data indicate that the topmost surface region of the as-cast films of the copolymer is composed of nearly 100% PDMS.

Annealing the as-cast samples increases the PDMS concentration in the topmost region. Thus, the surface of annealed copolymers (120 °C for 15 minutes) with a 10K PDMS segmental molecular weight consists of almost pure PDMS.

Segmental depth profiles were constructed from ESCA data. The profile typically contains a maximum and can be described by either a summation of step functions or a compound Gaussian distribution. The existence of a maximum indicates a PDMS deficient region beneath the PDMS enriched region. Annealing increases the thickness of both regions.

It has been demonstrated that both the length of the soft segments and the interactions among the hard segments affect the phase separation in the surface region. Long soft segments amplify entropically driven phase separation, and increased hydrogen bonding in hard segments augments the enthalpic driving force for phase separation.

Acknowledgment: This research was supported in part by the Office of Naval Research.

References

1. Brady, R. F.; Griffith, J. R.; Love, K. S.; Field, D. E. *J. Coatings Tech.* **1987**, *59*, 113.
2. Ho, T.; Wynne, K. J. *Macromolecules* **1992**, *25*, 3521.
3. McCarthy, T.; Ho, T.; Wynne, K. J. unpublished results.
4. Ho, T.; Wynne, K. J.; Nissan, R. *Macromolecules* **1993**, *26*, 7029.
5. Chen, X.; Gardella, J. A., Jr. *Polym. Prepr. Am Chem. Soc. Div. Polym. Chem.* **1992**, *33(2)*, 312.
6. Chen, X.; Gardella, J. A., Jr.; Kumler, P. L. *Macromolecules*, **1993**, 26, 3778.

7.a Schmitt, R. L.; Gardella, J. A., Jr.; Magill, J. H.; Salvati, L., Jr.; Chin, R. L. *Macromolecules*, **1985**, *18*, 2675.

7.b. Mittlefehldt, E. R.; Gardella, J. A., Jr. *Appl. Spectrosc.* **1989**, *43*, 1172.

8. Chen, X.; Lee, H. F.; Gardella, J. A., Jr. *Macromolecules* **1993**, *26*, 4601.
9. Chen, X.; Gardella, J. A., Jr.; Kumler, P. L. *Macromolecules*, **1992**, *25*, 6621.
10. Chen, X.; Gardella, J. A., Jr.; Kumler, P. L. *Macromolecules*, **1992**, *25*, 6631.
11. Thomas, H. R.; O'Malley, J. J. *Macromolecules*, **1979**, *12*, 323.
12. Coulon, G.; Russell,T. R.; Deline, V. R.; Green, P. F. *Macromolecules*, **1989**, *22*, 2581.

13. Clark, D. T. *Advances in Polymer Sciences*, 1977, *24*, 126.

14. Pijolat, M.; Hollinger, G. *Surf. Sci.* **1981**, *105*, 114.

15. Iwasaki, H; Nishitani, R; Nakamura, S *Jpn. J. Appl. Phys.* **1978**, *17*, 1519.

16. Holloway, P. H.; Bussing, T. D. *Surf. Interface Anal.* **1992**, *18*, 251.

17. Nefedov, V. I.; Baschenko, O. A. *J. Electron Spectrosc. Relat. Phenom.* **1988**, *47*, 1.

18. Tyler, B. J.; Castner, D.G.; Ratner, B. D. *Surf. Interface Anal.* **1989**, *14*, 443.

19. Jisl, R. *Surf. Interface Anal.* **1990**, *15*, 719.

20. Vargo, T. G.; Gardella, J. A., Jr. *J. Vac. Sci. Technol.* **1989**, *A7*, 1733.

21. Seah, M. P.; Dench, W. A. *Surf. Interf. Anal.* **1979**, *1*, 2.

22. Seinfeld, J. H.; Lapidus, L. *Mathematical Methods in Chemical Engineering, v.3 Process Modeling, Estimation, and Identification;* Prentice-Hall, Inc.: Englewood Cliffs, N. J., 1974; p 383.

23. Wu, S. *Polymer Interface and Adhesion;* Marcel Dekker: New York, 1982; p 184.

24. In a companion study by GPC, it was found that annealing at 120°C for two hours has insignificant effects on the average molecular weights of the current copolymers.

Table I Molecular Weights of the Segmented Copolymers

No.	Sample ID	PDMS MW[a]	Reaction Stoichiometry PDMS: IPDI: BDM	Copolymer MW[b] M_w	M_n	M_w/M_n
1	PDMS1K-IP-B0	1,000	1 : 1 : 0	16,700	12,000	1.4
2	PDMS1K-IP-B0.5	1,000	2 : 3 : 1	17,600	11,800	1.5
3	PDMS2.4K-IP-B0	2,400	1 : 1 : 0	65,000	30,700	2.1
4	PDMS2.4K-IP-B1	2,400	1 : 2 : 1	76,500	27,700	2.8
5	PDMS2.4K-IP-B2	2,400	1 : 3 : 2	42,700	19,100	2.2
6	PDMS10K-IP-B0	10,000	1 : 1 : 0	109,000	54,500	2.0
7	PDMS10K-IP-B2	10,000	1 : 3 : 2	81,200	29,200	2.8
8	PDMS27K-IP-B2	27,000	1 : 3 : 2	198,000	149,000	1.3

(a). Amino terminated siloxane oligomers with molecular weight provided by the supplier.

(b). Polymer molecular weight determined by GPC.

Table II Conversion Formulas between Atomic Ratio and Segment Weight Fraction for the Copolymers

Sample	Formula[a]
1	$X = \frac{[\ 956 - 956\ (N/C)\ ]\ 100}{956 + 949\ (N/C)}$
2	$X = \frac{[\ 4780 - 21032\ (N/C)\ ]\ 100}{4780 - 8012\ (N/C)}$
3	$X = \frac{[\ 2362 - 7086\ (N/C)\ ]\ 100}{2362 - 2768\ (N/C)}$
4	$X = \frac{[\ 3534 - 18896\ (N/C)\ ]\ 100}{3543 - 8458\ (N/C)}$
5	$X = \frac{[\ 2362 - 15353\ (N/C)\ ]\ 100}{2362 - 7074\ (N/C)}$
6	$X = \frac{[\ 9984 - 29953\ (N/C)\ ]\ 100}{9984 - 6203\ (N/C)}$
7	$X = \frac{[\ 19968 - 129792\ (N/C)\ ]\ 100}{19968 - 63073\ (N/C)}$
8	$X = \frac{[\ 1000 - 6500\ (N/C)\ ]\ 100}{1000 - 3197\ (N/C)}$

(a). (N/C) is the ratio of the peak area of nitrogen atoms to the peak area of carbon atoms measured by ESCA.

Table III How The Carbon Densities Calculated

The calculation was based on the following data.

	Density(g/ml)	MW	# of C/MW	mole of C/liter
PDMS	0.93-0.97	74	2	25.7
IPDI	1.049	222	11	52.0
BDM	1.175*	138	8	

Average values for hard segments.

BDM:IPDI	Density(g/ml)	MW	# of C/MW	mole of C/liter
0:1	1.05	254	11	45.5
1:3	1.07	836	41	52.5
1:2	1.08	614	30	52.8
2:3	1.08	974	49	54.3

* extrapolated from density data for benzene and benzyl alcohol.

Table IV Coefficients η, σ, And γ For Each Polymer

Polymer	η	σ	γ
PDMS1K-IP-B0	45.5	28.7	0.364
PDMS1K-IP-B0.5	52.5	28.7	0.244
PDMS2.4K-IP-B0	45.5	27.0	0.364
PDMS2.4K-IP-B1	52.8	27.0	0.200
PDMS2.4K-IP-B2	54.3	27.0	0.163
PDMS10K-IP-B0	45.5	26.0	0.364
PDMS10K-IP-B2	54.3	26.0	0.163
PDMS27K-IP-B2	54.3	25.8	0.163

Table V PDMS Wt% of the As-cast Samples From THF Solutions

No.	Sample ID	PDMS Wt%				
		θ = 10°	15°	30°	90°	Bulk
1	PDMS1K-IP-B0	93.6±1.3	90.6±2.3	86.8±2.2	83.5±1.3	79.0
2	PDMS1K-IP-B0.5	88.6±2.3	83.9±0.4	77.2±1.2	71.4±1.0	68.8
3	PDMS2.4K-IP-B0	96.8±0.8	94.4±1.0	92.4±0.2	90.6±0.3	90.3
4	PDMS2.4K-IP-B1	95.0±2.7	92.1±1.4	83.9±1.8	79.4±1.6	79.4
5	PDMS2.4K-IP-B2	88.0±1.8	84.9±1.6	78.5±1.5	72.5±0.9	70.8
6	PDMS10K-IP-B0	98.9±0.7	98.5±0.5	97.7±0.1	97.0±0.6	97.5
7	PDMS10K-IP-B2	97.7±0.5	97.0±1.4	93.5±1.0	90.0±1.5	91.1
8	PDMS27K-IP-B2	100.±0.0	99.1±0.9	98.0±0.7	97.2±1.3	96.5

Table VI PDMS Wt% of the Copolymer Samples, Annealed at 120°C for 15 Minutes

No.	Sample ID	PDMS Wt%				
		θ = 10°	15°	30°	90°	Bulk
1	PDMS1K-IP-B0	93.7±0.2	90.8±0.8	87.3±0.5	84.0±0.6	79.0
2	PDMS1K-IP-B0.5	88.6±2.2	81.9±1.6	75.2±0.6	69.7±0.4	68.8
3	PDMS2.4K-IP-B0	97.1±0.5	95.4±1.0	92.5±0.4	91.3±0.4	90.3
4	PDMS2.4K-IP-B1	94.8±1.3	91.9±0.8	85.4±0.5	81.2±0.4	79.4
5	PDMS2.4K-IP-B2	93.6±1.8	89.5±0.3	79.8±0.2	74.1±0.3	70.8
6	PDMS10K-IP-B0	99.9±0.1	99.5±0.2	98.5±0.7	97.1±0.2	97.5
7	PDMS10K-IP-B2	99.4±0.8	98.5±0.2	96.2±1.9	93.2±1.0	91.1
8	PDMS27K-IP-B2	100.±0.0	99.9±0.0	99.1±0.1	97.6±0.2	96.5

Table VII PDMS Wt% of the Copolymer Samples, Annealed at 120°C for Two Hours

Sample No.	ID	PDMS Wt%					
	θ =	10°	15°	30°	90°	90°#	Bulk
1	PDMS1K-IP-B0	91.9±2.1	91.2±0.9	86.5±0.3	86.5±0.3	83.7±1.2	79.0
2	PDMS1K-IP-B0	89.1±2.0	88.7±6.5	80.3±0.4	73.6±0.2	72.5±1.2	68.8
3	PDMS2.4K-IP-B0	98.5±1.2	98.4±0.8	94.3±0.1	91.9±1.1	89.2±1.1	90.3
4	PDMS2.4K-IP-B1	93.1±1.8	91.6±0.2	87.4±2.0	80.3±0.7	79.1±0.5	79.4
5	PDMS2.4K-IP-B2	94.2±4.5	92.7±2.4	80.0±0.8	73.1±2.1	69.2±0.4	70.8
6	PDMS10K-IP-B0	100.±0.0	100.±0.0	99.1±0.1	98.5±0.4	97.6±0.2	97.5
7	PDMS10K-IP-B2	100.±0.0	99.3±0.2	97.2±1.2	91.4±0.9	89.0±4.2	91.1
8	PDMS27K-IP-B2	100.±0.0	100.±0.0	98.9±0.7	97.6±0.4	87.0±1.8	96.5

With Ti anode X-ray source.

Table VIII Concentration Depth Profile Data for Copolymer PDMS2.4K-IP-B2 before Annealing

Take Off Angle	10°	15°	30°	90°
Upper Uncertainty Limit	37.4	29.0	20.5	16.2
C/N (ESCA Data)	32.2	26.2	19.3	15.7
Lower Uncertainty Limit	28.4	24.0	18.2	15.3
C/N (Discrete Model)	36.0	27.6	19.1	15.4
C/N (Continuous Model)	32.6	26.2	19.1	15.8

Parameters for the depth profile of the hard segment.

1. Discrete model

δ_1	δ_2	$v(\infty)$	h_1	h_2	h_3	h_4	h_5	h_6	h_7	h_8
.30	.35	.292	.2	.8	1.2	1.5	1.2	1.0	1.0	1.0

2. Continuous model

y_1	l_1	σ_1	σ_2
1.30	1.00	0.50	0.38

Table IX Concentration Depth Profile Data for Copolymer PDMS2.4K-IP-B2, Annealed at 120°C for 15 Minutes

Take Off Angle	10°	15°	30°	90°
Upper Uncertainty Limit	79.2	37.4	20.5	16.7
C/N (ESCA Data)	57.8	36.4	20.3	16.5
Lower Uncertainty Limit	45.7	35.4	20.2	16.4
C/N (Discrete Model)	55.4	36.6	20.5	14.9
C/N (Continuous Model)	55.6	36.9	20.4	14.6

Parameters for the depth profile of the hard segment.

1. Discrete model

δ_1	δ_2	$v(\infty)$	h_1	h_2	h_3	h_4	h_5	h_6	h_7	h_8
.31	.35	.292	.1	.6	1.2	1.8	1.9	1.5	1.1	1.0

2. Continuous model

y_1	l_1	σ_1	σ_2
1.99	1.30	0.50	0.48

Table X Concentration Depth Profile Data for Copolymer PDMS2.4K-IP-B2, Annealed at 120°C for Two Hours

Take Off Angle	10°	15°	30°	90°
Upper Uncertainty Limit	272.6	74.5	21.3	17.1
C/N (ESCA Data)	63.4	51.0	20.5	16.0
Lower Uncertainty Limit	37.0	39.1	19.8	15.1
C/N (Discrete Model)	97.0	47.2	22.7	16.0
C/N (Continuous Model)	61.2	40.4	21.9	15.3

Parameters for the depth profile of the hard segment.

1. Discrete model

δ_1	δ_2	$v(\infty)$	h_1	h_2	h_3	h_4	h_5	h_6	h_7	h_8
.34	.35	.292	0.	.7	1.3	1.8	1.4	1.1	1.0	1.0

2. Continuous model

y_1	l_1	σ_1	σ_2
1.82	1.30	0.50	0.64

Table XI Keys to Read Concentration Depth Profile Data

C/N (ESCA Data): the average of three measurements.

Upper Uncertainty Limit: the average plus one standard deviation based on three measurements.

Lower Uncertainty Limit: the average minus one standard deviation based on three measurements.

C/N (Discrete Model): calculated from the discrete model (see text for details of this model) with the optimal parameters.

C/N (Continuous Model): calculated from the continuous model (see text for details of this model) with the optimal parameters.

Parameters for the Discrete Model
The depth profile is described with a series of eleven numbers. These numbers are used to specify the starting position and hight of each constituent step function. (Refer to profiles in Figure 8 for illustration.) The first two numbers are the staggered distances between two step functions. In this study, the distances staggered were kept alternating between two values. For example, the staggered distances between two consecutive step functions for the profile shown in Figure 8 are 0.30 and 0.35 λ, alternately. The third number is the bulk value for the volume fraction of the hard segment, which is also equal to the sum of the heights of all the nine step functions. The forth number is the height of the first step function, the fifth number is the sum of the heights of the first and the second step functions. Similarly, each subsequent number is the sum of the previous number and the height of an additional step function. (From the forth to the eleventh number, the value is normalized with respect to the bulk volume fraction, i.e. the third number.)

Parameters for the Continuous Model
The depth profile is described with a four-parameter compound Gaussian distribution model of the form

$$y(l) = y_1 \, \mathrm{Exp}[-0.5 \, (l - l_1)^2/\sigma_1^2] \qquad l \le l_1$$
$$= 1 + (y_1 - 1) \, \mathrm{Exp}[-0.5 \, (l - l_1)^2/\sigma_2^2] \qquad l > l_1$$

where y is $v(l)/ v(\infty)$, $v(\infty)$ the bulk value of v, the volume fraction of the hard segment; l is the distance from surface divided by the escape depth. The four parameters are y_1, the maximum y value of the profile; l_1, location of the maximum of the profile; σ_1, and σ_2 characterize the shape of the profile to the left and to the right of the maximum, respectively.

Figure Captions

Figure 1. Structure of PDMS-PU segmented copolymers.

Figure 2. PDMS concentration in the surface region measured by ESCA for three copolymers. The distance between the horizontal bar and the top of the column represents one standard deviation. Data series: A, PDMS1K-IP-B0; B, PDMS2.4K-IP-B0; and C,PDMS10K-IP-B0.

Figure 3. PDMS concentration in the surface region measured by ESCA for three copolymers. The distance between the horizontal bar and the top of the column represents one standard deviation. Data series: A, PDMS2.4K-IP-B2; B, PDMS10K-IP-B2; and C,PDMS27K-IP-B2.

Figure 4. PDMS concentration in the surface region measured by ESCA for three copolymers. The distance between the horizontal bar and the top of the column represents one standard deviation. Data series: A, PDMS2.4K-IP-B0; B, PDMS2.4K-IP-B1; and C,PDMS2.4K-IP-B2.

Figure 5. PDMS concentration in the surface region measured by ESCA for two copolymers of similar bulk PDMS concentration. The distance between the horizontal bar and the top of the column represents one standard deviation. Data series: A, PDMS10K-IP-B2; and B, PDMS2.4K-IP-B0.

Figure 6. PDMS concentration in the surface region measured by ESCA for the copolymer PDMS10K-IP-B2 under different thermal treatments. The distance between the horizontal bar and the top of the column represents one standard deviation. Data series: A, as-cast; B, annealed at 120°C for 15 min.; and C, for two hours.

Figure 7. Concentration depth profiles for the hard segment in as-cast films of copolymer PDMS2.4K-IP-B2. Profiles: A, constructed based on a continuous model; B, constructed based on a discrete model; and (■) data measured by ESCA.

Figure 8. Concentration depth profiles of the hard segments in the surface region for the copolymer PDMS2.4K-IP-B2 under different thermal treatments. The profiles are constructed based on a discrete model. Curves: A, as-cast; B, annealed at 120°C for 15 minutes; and C, for two hours.

Figure 9. Concentration depth profiles of the hard segments in the surface region for the copolymer PDMS2.4K-IP-B2 under different thermal treatments. The profiles are constructed based on a continuous model. Curves: A, as-cast; B, annealed at 120°C for 15 minutes; and C, for two hours.

Figure 10. v_N as a function of depth in the surface region for two copolymers. Curves: A, PDMS10K-IP-B0 as-cast; B, PDMS10K-IP-B2 as-cast; C, PDMS10K-IP-B0 annealed at 120°C for 15 minutes; and D, PDMS10K-IP-B2 annealed at 120°C for 15 minutes.

Figure 11. v_N as a function of depth in the topmost surface region for two copolymers. Curves: A, PDMS10K-IP-B0 as-cast; B, PDMS10K-IP-B2 as-cast; C, PDMS10K-IP-B0 annealed at 120°C for 15 minutes; and D, PDMS10K-IP-B2 annealed at 120°C for 15 minutes.

Figure 12. v_N as a function of depth in the topmost surface region for three copolymers. Curves: A, PDMS2.4K-IP-B2 as-cast; B, PDMS10K-IP-B2 as-cast; C, PDMS27K-IP-B2 as-cast; D, PDMS2.4K-IP-B2 annealed at 120°C for 15 minutes; E, PDMS10K-IP-B2 annealed at 120°C for 15 minutes; and F, PDMS27K-IP-B2 annealed at 120°C for 15 minutes.

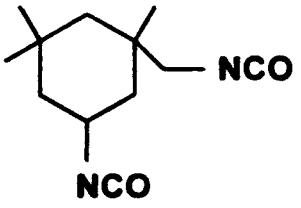

IPDI

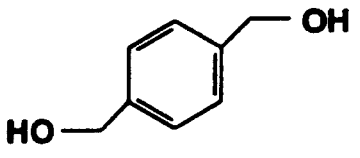

BDM

$H_2N(CH_2)_3$-[$Si(CH_3)_2$-O]$_n$-$Si(CH_3)_2$-$(CH_2)_3NH_2$

PDMS Oligomer

-[-PDMS-[(IPDI)$_m$-(BDM)$_{m-1}$]-]$_p$-

PDMS-PU Segmented Copolymer

Fig 1

Fig 1

Figure 2

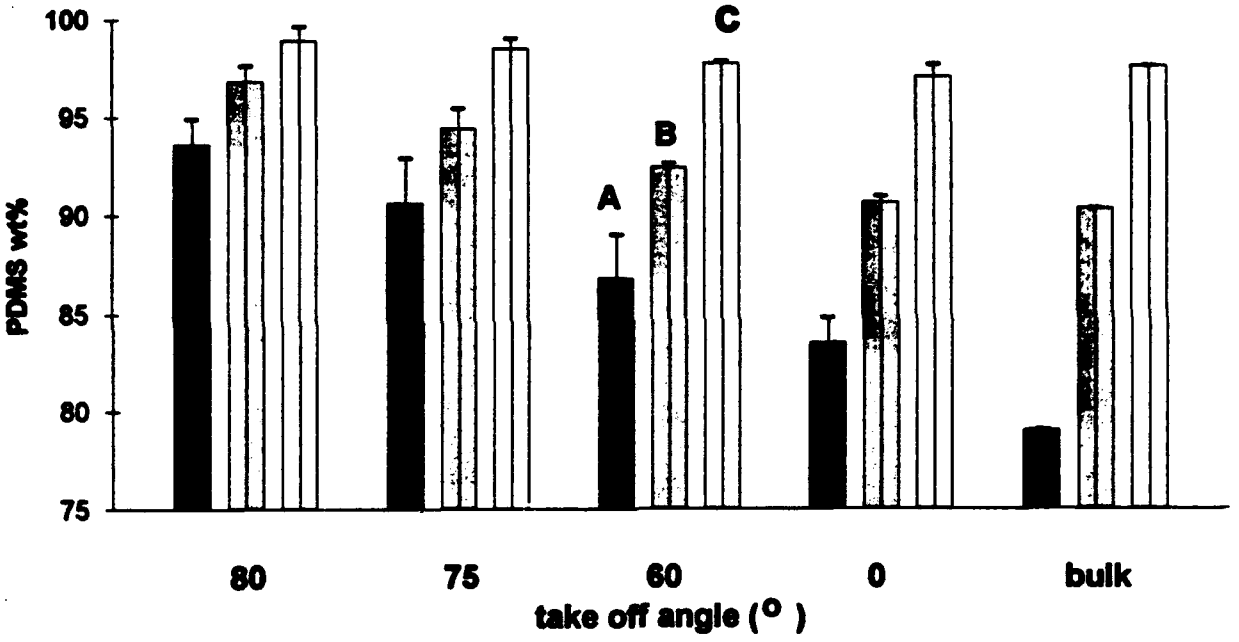

Figure 3

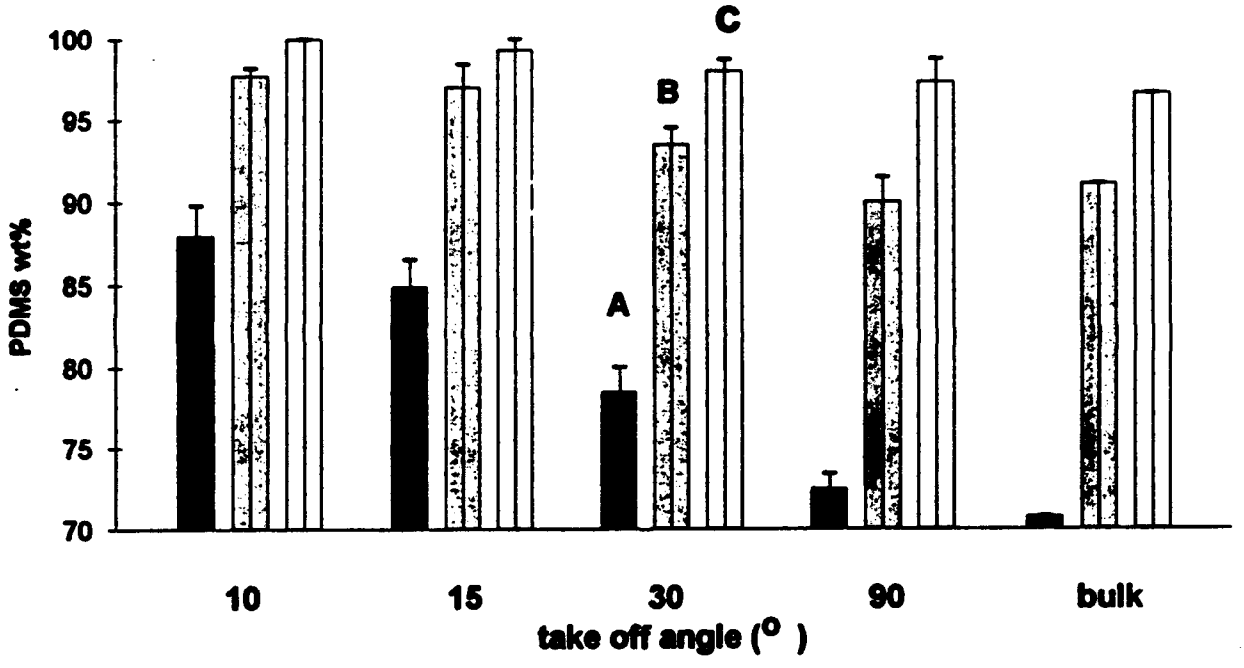

Figure 4

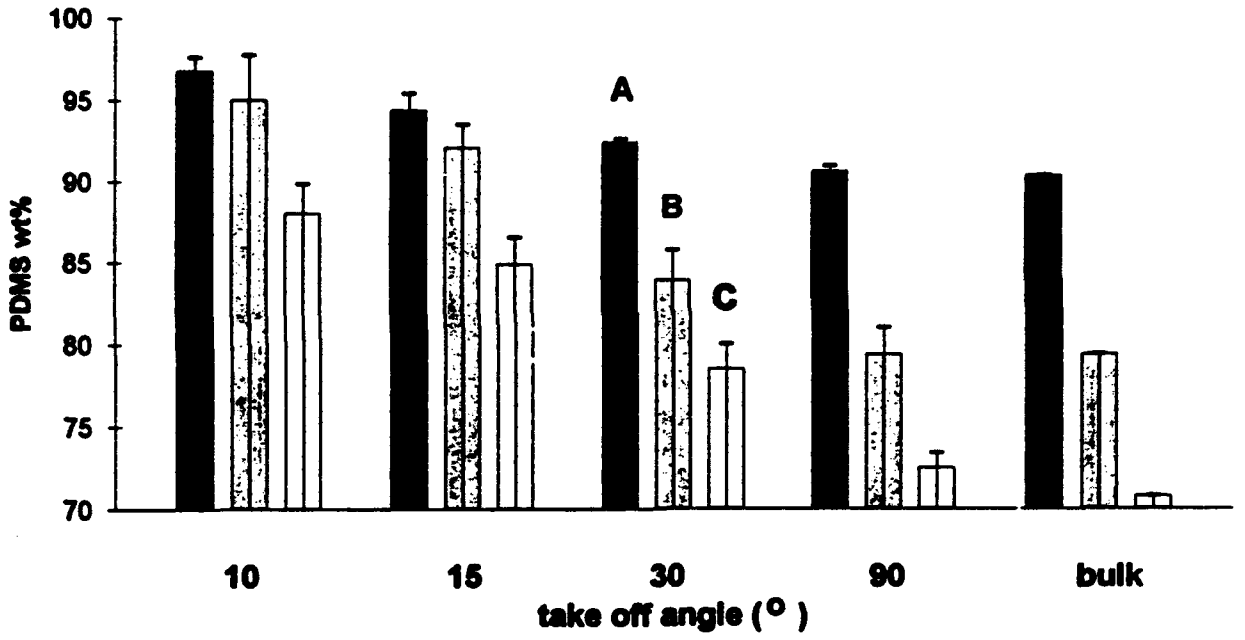

Figure 6

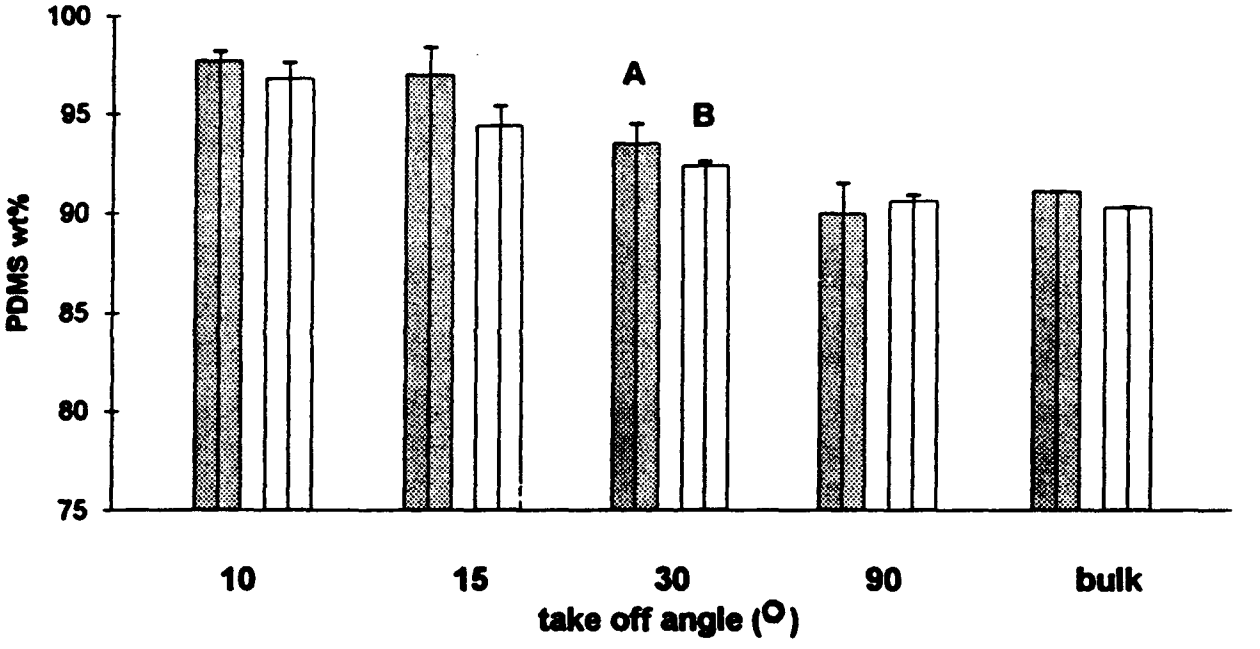

Figure 6

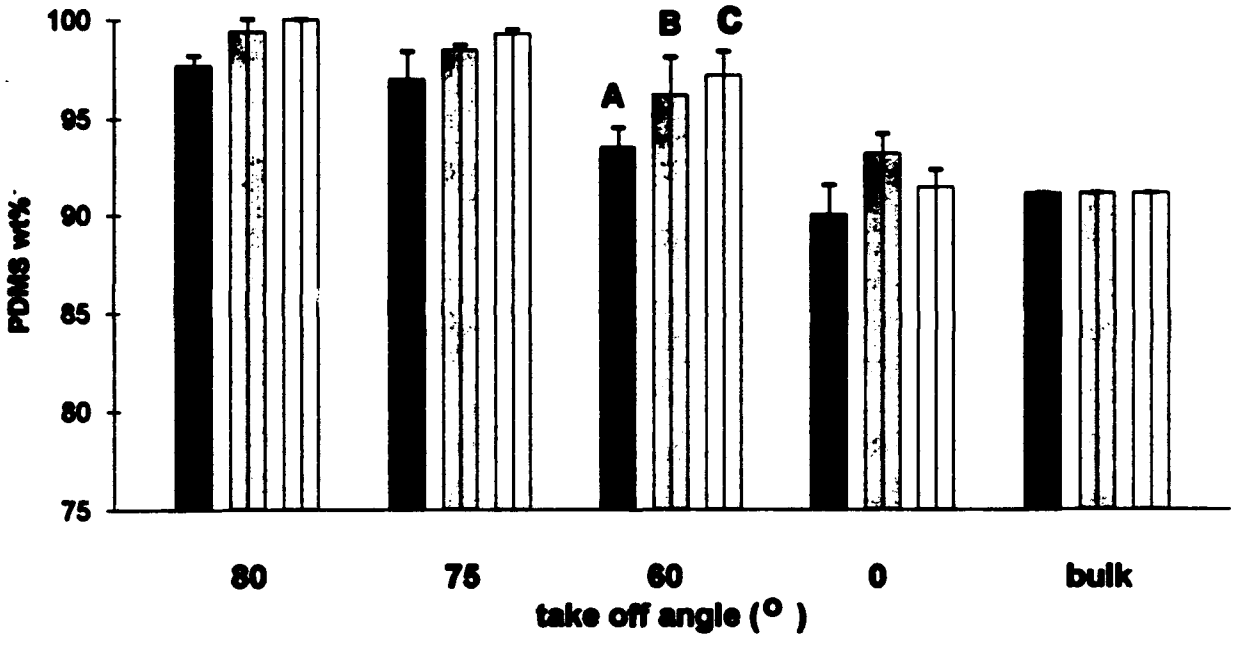

Figure 7

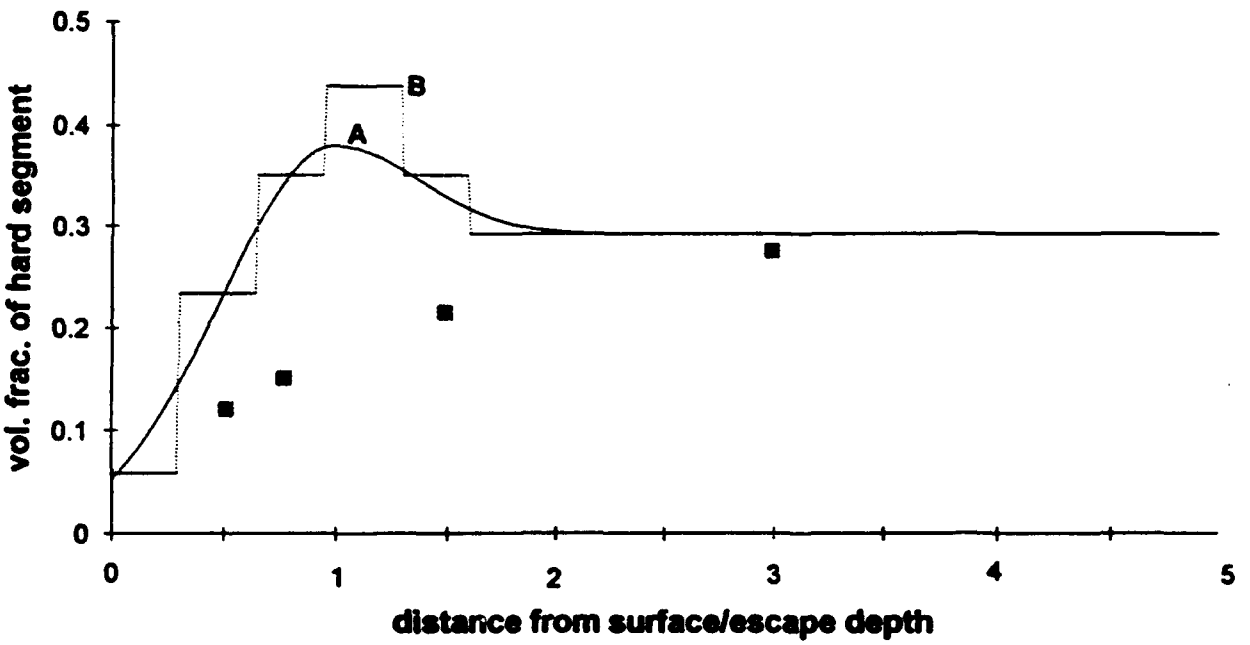
vol. frac. of hard segment
0.5
0.4
0.3
0.2
0.1
0
B
A
0
1
2
3
4
5
distance from surface/escape depth

Figure 8

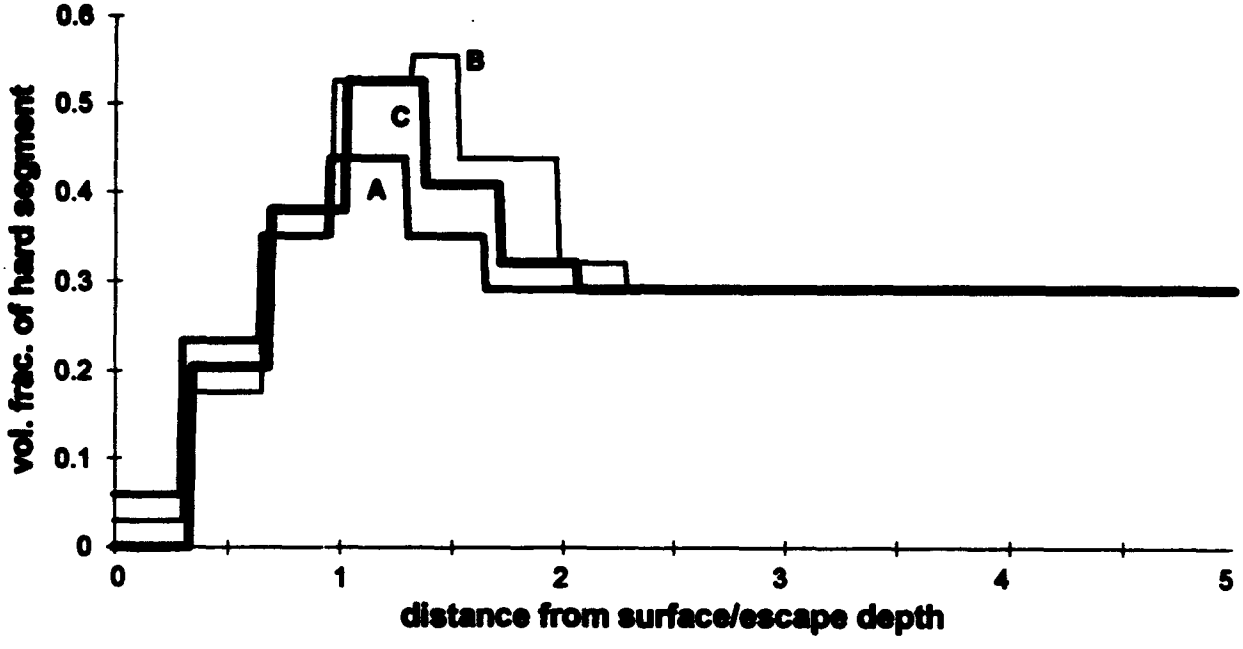
0.6
0.5
0.4
0.3
0.2
0.1
0
vol. frac. of hard segment
B
C
A
0
1
2
3
4
5
distance from surface/escape depth

Figure 9

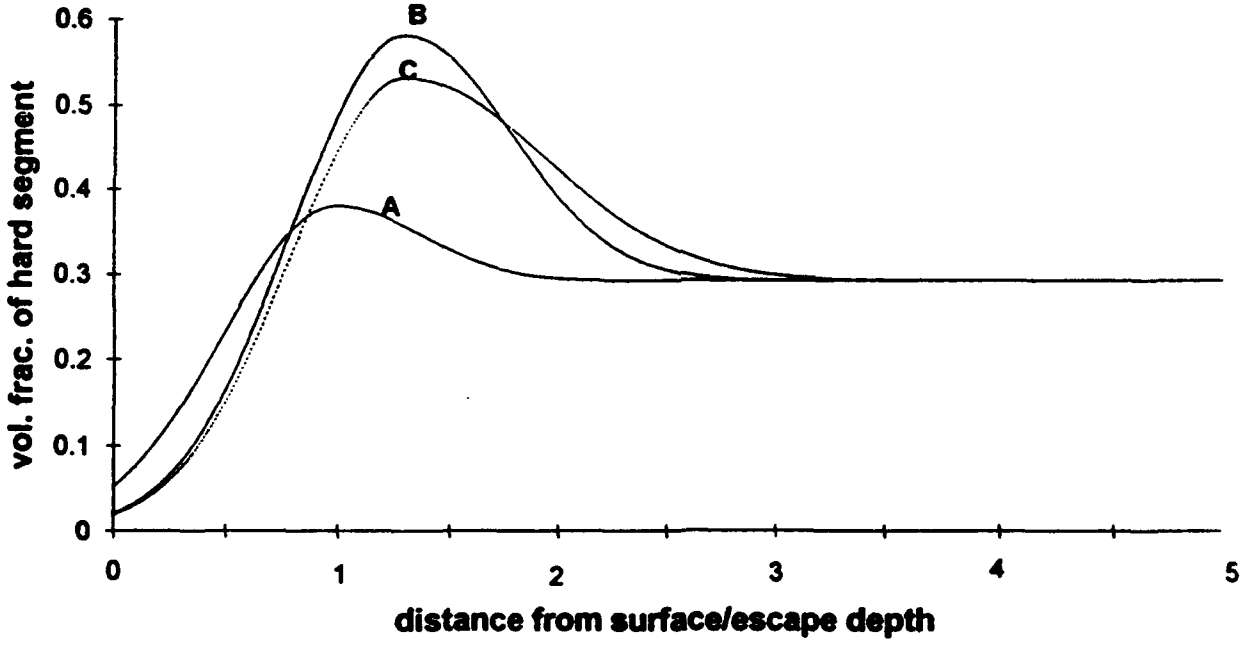
vol. frac. of hard segment
0.6
0.5
0.4
0.3
0.2
0.1
0
B
C
A
0
1
2
3
4
5
distance from surface/escape depth

Figure 10

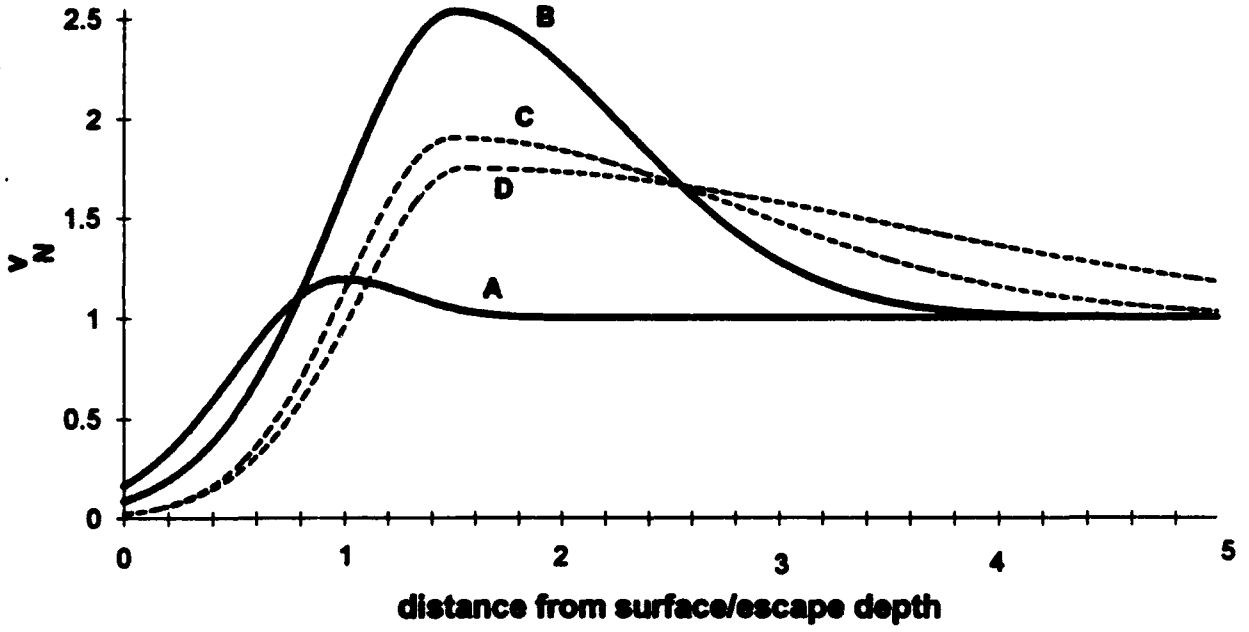
2.5
2
1.5
1
0.5
0
>z
B
C
D
A
0
1
2
3
4
5
distance from surface/escape depth

Figure 11

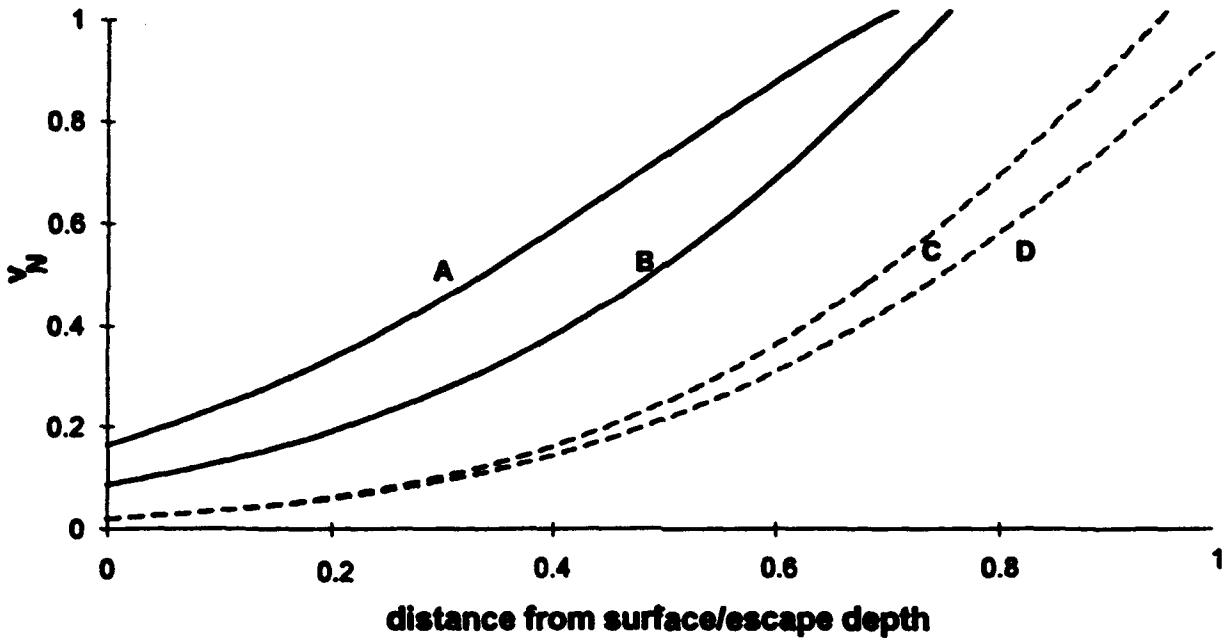
1
0.8
0.6
0.4
0.2
0
0
0.2
0.4
0.6
0.8
1
A
B
C
D
distance from surface/escape depth

Figure 1b 12

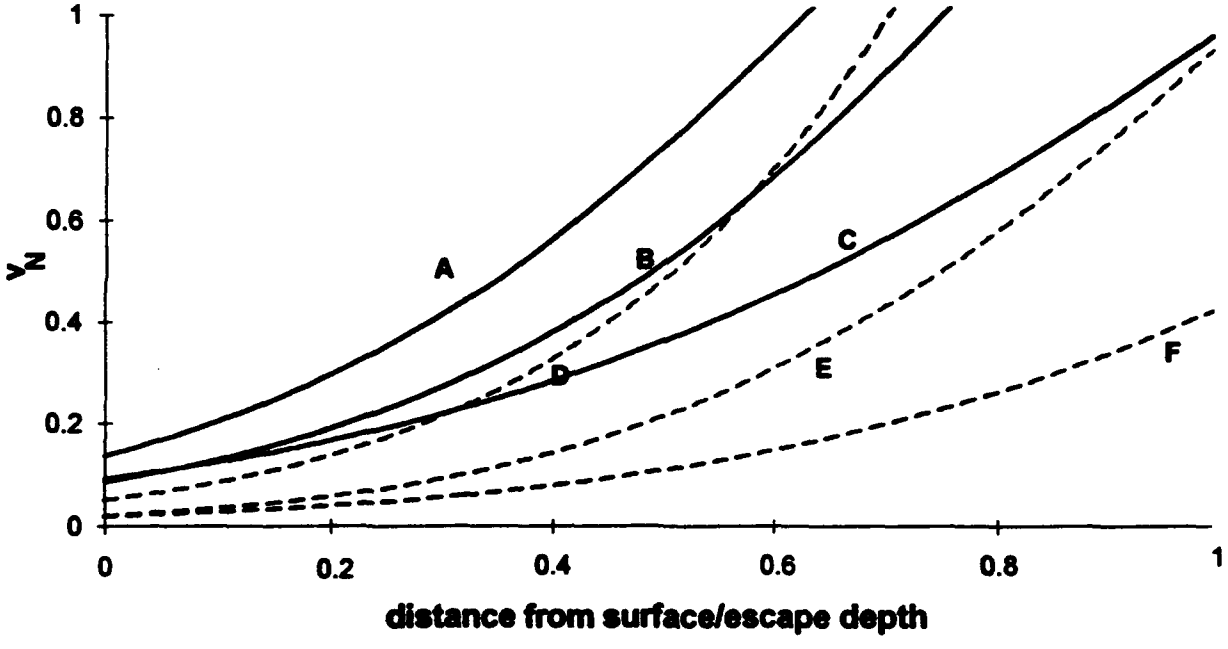
1
0.8
0.6
0.4
0.2
0
0
0.2
0.4
0.6
0.8
1
A
B
C
D
E
F
distance from surface/escape depth

Surface Modification Studies of Polymer blends

Jiaxing Chen, Xin Chen,
and Joseph A. Gardella, Jr.*

Department of Chemistry
State University of New York at Buffalo
Buffalo, NY 14214

Introduction

To obtain a desired surface property of polymeric materials, different surface modification techniques have been employed such as plasma treatment[1,2], surface grafting[3,4], chemical reaction[1,5], vapor deposition of metals[6] and surface segregation of polymer blends[7]. It has been shown that if a low surface tension property is desired, surface segregation by blending a small amount of block copolymer with a segment of low tension block into the homopolymer is a great advantage[8,9]. In our previous studies[7], it has demonstrated that to modify the surface energies of polystyrene (PS) and poly (a-methylstyrene), a small amount of a block copolymer of poly(dimethylsiloxane) and a segment the same as the homopolymer blended into the bulk homopolymer effectively changed the composition of the polymer surface. The enrichment of the segment with lower surface tension at the topmost region lowered the surface energy of the materials. The extent and effectiveness of surface segregation, however, depend on many factors such as the relative molecular weight of the two segments in the binary copolymer[7,10], the architecture of the copolymer[11,12], and the history of manufacturing of the polymer films[13]. Annealing and solvent effect are two important influencing factors. In this report, studies on the architecture effect of the copolymer and annealing effect are presented.

Experimental

Homopolymers employed in this studies are narrow distribution standards purchased from Scientific Polymer Products. Block copolymers are narrow distribution copolymer products received

from donations. Polymer blends were made by dissolving the polymers in solvents selected and films were casted directly into aluminum dishes. These were allowed to Air dry before further treatment. Vacuum oven drying at room temperature for at least one day was conducted to make solvent free films. For annealing studies, annealing was conducted in a vacuum dry oven at different temperatures.

Surface composition was determined by Angle-dependent ESCA and ATR-FTIR to get the details at different depth profile. The ESCA measurement was described in the pervious papers[11,14-15]. ATR-FTIR measurement was performed on a Nicolet Magna IR-550 with a DTGS-KBr detector at a resolution of 4 cm^{-1}. The accessary for ATR is Hartick Tmpra and the prisms are Ge single pass parrellpiped, 50*10*3 mm with face cut of 45° and 60°. A sampling depth of 2.4 - 3.0 μm is estimated from the air surface for the IR absorption bands between 700 and 800 cm^{-1}.

Results and Discussion

Binary blends investigated are grouped according to the architectures and the dose amount of the copolymer blended. Copolymers of different architectures are listed in table 2 for comparison.

PS-PDMS/PS Blends The AB/A binary blends are listed in Table 1 and the results in Table 3. The first 3 groups in Table 1 are the same copolymer blended with PS of different molecular weights and different copolymer doses. The results shown in Table 3 demonstrates that a higher molecular weight of the homopolymer gives a better surface segregation, while a heavier copolymer dose does not influence the surface segregation much. By sample group 7 and 8, the amount of copolymer blended increasing with the same homopolymer and copolymer combination, surface composition results show that the DMS concentrations segregated into the top-most region are very close although the bulk concentration blended increased significantly. The molecular weight of the copolymer and the relative molecular weight of the two blocks are expected to influence the surface segregation significantly. The 4th to 6th groups in Table 1

shows the architecture influence on surface segregation. The results suggests that on the same DMS percentage, AB diblock copolymer allows better segregation than triblock copolymers.

From Table 4 we can see that the AB binary copolymer has a better segregation ability. Sample 22 has the lowest bulk percentage of DMS segment, but gives higher surface concentration.

Annealing effect Annealing is a process of thermal movement of segments in the system before equilibrium under certain thermal environment. For the systems that thermal equilibrium is easily reached under lower temperature, annealing will not show significant change. For the systems in which thermal motion of segment are highly restricted, however, hence the thermal equilibrium of such a system requires a longer time. Annealing at higher temperatures offer higher thermal motion energies to segment in the bulk material, so more change should be able to observe to these system. For the copolymer systems investigated, AB diblock copolymer possesses better mobility than the triblock copolymers, and lower molecular weight offer better mobility of the segments than higher molecular weight. The surface composition measurement results indicate that the BAB triblock copolymer shows higher composition change after annealing treatment. Table 4 shows the annealing effect on surface segregation for the pure copolymers. Sample 24 gives the highest composition change on the surface composition before and after annealing, however, sample 22's surface composition of both before and after annealing imply that AB type copolymer possesses better segregation ability. Sample 22 has the lowest overall DMS concentration. The surface concentration before annealing has already shown high degree of surface segregation. The effect of annealing on binary polymer blends is under investigation currently.

Acknowledgement Financial support from NSF Polymers Program (9303032) is greatly appreciated.

References

1. Vargo, T. G.; Thompson, P. M.; Gerenser, L. J.; Valentini, R. F.; Aebischer, P.; Hook, D. J.; Gardella, J. A, Jr. *Langmuir* 1992, *8*, 130.
2. Kim, C. Y.; Evans, J.; Goring, D. A. I. *J. Appl. Polym. Sci.* 1971, *15*, 1365.
3. Feng, X. D.; Sun, Y. H.; Qin, K. Y. *Macromolecules* 1985, *16*, 2105.
4. Liouni, M.; Touloupis, C.; Hadjichristidis, N.; Karvounis, S.; Marston, E. V. *J. Appl. Polym. Sci.* 1992, *45*, 2199.
5. Tsukada, M.; Goto, Y.; Freddi, G.; Shiozaki, H. *J. Appl. Polym. Sci.* 1992, *45*, 1189.
6. Silvain, J. F.; Ehrhardt, J. J.; Lutgen, P. *Thin Solid Films* 1991, *L5*, 195.
7. Xin Chen and Joseph A. Gardella, Jr. *Macromolecules* in press
8. Dwight, D. W.; McGrath, J. E.; Riffle, J. S.; Smith, S. D.; York, G. A. *J. Elec. Spec. Rel. Phen.* 1990, *52*, 457.
9. LeGrand, D. G.; Gaines, G. L., Jr. *Polym. Prepr. Am. Chem. Soc. Div. Polym. Chem.* 1970, *11*, 442.
10. Xin Chen and Joseph A. Gardella, Jr. *Macromolecules* in press
11. Xin Chen; J. A. Gardella, Jr. and P. L. Kumler, *Macromolecules* 1992, *25*, 6621.
12. Xin Chen; J. A. Gardella, Jr. and P. L. Kumler, *Macromolecules* 1992, *25*, 6631.
13. T. Ho; K. J. Wynne; and R. Nissan *Macromolecules*, in press
14. Chen, X.; Gardella, J. A., Jr.; Kumler, P. L. *Macromolecules* 1993, *26*, 3778.
15. Chen, X.; Lee, H. F.; Gardella, J. A., Jr. *Macromolecules* 1993, *26*, 4601.

QUANTITATIVE SURFACE ANALYSIS OF SOLVENT EFFECTS ON FILM FORMATION OF BPAC/DMS COPOLYMERS

Hengzhong Zhuang, Joseph A. Gardella, Jr.
Department of Chemistry, SUNY at Buffalo
Buffalo, NY 14214

Tai Ho, Kenneth J. Wynne
Chemistry Division, Office of Naval Research
Arlington, VA 22217-5660 and
Materials Chemistry Branch
Naval Research Laboratory
Washington, D.C. 20375-5000

Introduction

The study of minimal fouling coatings is an increasingly active research field, in which PDMS (polydimethylsiloxane) enriched films are one promising minimally adhesive surface[1]. It was found that compositional and morphological features play a crucial role in determining the effectiveness of minimal fouling. Various Silicon containing copolymer and polymer blends have been examined to meet the compositional requirement [1, 2]. Because of their properties of low surface energy, excellent mechanical strength and good adhesion to metal and other base materials, BPAC/DMS (bisphenol A polycarbonate and dimethylsiloxane) block copolymers are one minimally adhesive coating materials among others. In this study, we systematically investigated solvent and annealing effects on the surface composition of solution-cast films of BPAC/DMS copolymers by angle-resolved ESCA (Electron Spectroscopy for Chemical Analysis) and ATR-FTIR (Attenuated Total Reflectance).

Experimental

The samples were a series of BPAC/DMS block copolymers having a DMS block length of 20 and the following weight percent composition: 35/65, BPAC/DMS; 50/50, BPAC/DMS; and 75/25, BPAC/DMS [2, 3]. Six solvents with distinctive properties were selected, in particular, methylene dichloride, chloroform, carbon tetrachloride, tetrahydrofuran (THF), benzene and pyridine. Solutions (~0.5% w/w) were made and cast into

films in aluminum weighing pans. Half of the samples were annealed at 180°C for 17 hours. ATR results at 4 cm^{-1} resolution were obtained on a Magna-IR 550 spectrometer (DTGS detector) equipped with a Harrick Scientific Model X ATR attachment and Ge internal reflection element (face cut at 45°). Incident analysis angle of 45° was chosen to yield a sampling depth of approximately 1.6 um [4, 5]. ESCA results were obtained on a Model 5300 PHI-ESCA (Mg Ka as X-ray source) at take-off angles of 45° and 90° which yield sampling depths of approximately 50 Å and 100 Å [6], respectively.

Results and Discussion

ESCA data were originally extracted in the form of atomic percentage with Phi Version 2 ESCA software [7]. They were transformed into mass percentage of DMS (see Table 1) according to the following equation [2]:

Mass % DMS = [1187.2*(Si/C)]/[254.3+678.6*(Si/C)]

Data in Table 1 shows that there is a compositional distribution gradient (from 50 Å to 100 Å in depth) with DMS at a higher percentage of DMS on the surface than in the bulk, i.e., DMS enriched in the air-solid interface. The degree of DMS enrichment depends on solvents used to prepare the solution from which films were cast.

It is complicated to rationalize a quantitative relationship between film structure and solvent properties. But the following qualitative conclusions can be drawn:

(1) Carbon tetrachloride is not a good solvent for BPAC/DMS copolymer. In other words, the interaction between polymer chain and carbon tetrachloride is not as strong as when good solvent is involved. The polymer chains in solution tend to aggregate instead of moving freely to the surface forming a lower energy surface with excessive DMS. Therefore, there is less excessive DMS on the surface of films made with carbon tetrachloride (see Table 1).

(2) Among good solvents, the volatility (or

boiling point) varies. For example, methylene dichloride has a boiling point of 39.8°C while pyridine of 115°C. It is predicted that BPAC/DMS copolymer film cast with methylene dichloride will be less stable thermodynamically than that with pyridine, because polymer chains in the former case have less time to rearrange themselves into a thermodynamically stable state as solvent evaporating. However, on annealing, DMS in the films will move onto the surface to form a lower energy surface (more stable state). Subsequently, more DMS should be detected. In Table 1, for films cast from methylene dichloride, DMS is 84.0%(Wt) within 50Å (45°) and 82.7%(Wt) within 100Å (90°) in depth, while the corresponding DMS percentages of the films cast from pyridine are very close, before and after annealing. This indicates that films cast with methylene dichloride is less stable than that cast with pyridine.

(3) A further interesting phenomenon was found when all the ESCA data for annealed films were examined as a whole. The compositional data for annealed films were not the same even after they were annealed at 180°C, over 20°C higher than the highest T_g of copolymer components, for 17 hours. Such a harsh condition was employed to ensure the film reached a real thermodynamic equilibrium state. It is worth noting herein that there was no significant degradation observed by comparing FTIR spectra for samples before and after such a long time annealing. Since the migrating element in the annealing process (at temperature far below melting point) was a polymer segment not the entire polymer chain, the large scale morphology remains while polymer segments rearranged locally. Thus, the peculiar film structure with a certain solvent is preserved. This so-called solvent "memory" effect will be further illustrated by ATR-FTIR data (Table 2).

ATR-FTIR was used to composition at much deeper depth. ATR-FTIR spectra were deconvolved by Maximum Likelihood Restoration run under Square Tools, Lab Calc (Galactic Industries Corp.,

Salem, New Hampshire). The peak area ratio of 1194 cm^{-1} (indicative of BPAC) to 1260 cm^{-1} (indicative of DMS) [8] was used to quantify DMS composition in the film with the composition calibration curve prepared from seven transmission FTIR spectra for BPAC/DMS blends of known composition. The data were tabulated in Table 2 in which the weight percentage of DMS was an average value over an entire detection range (typically 1.6 um). There was no significant distinction between annealed and not annealed cases in terms of DMS composition. This is further evidence that annealing can not change films made with different solvents into the same morphology.

Reference

(1) T. Ho; Wynne, K. J. Macromolecules 1992, 25, 3521
(2) X. Chen, Dissertation (Ph.D), Dept. of Chem. SUNY at Buffalo, 1993
(3) E. R. Mittlefehldt and J. A. Gardella, Jr., Appl. Spectrosc. 43, 1173 (1989)
(4) N. J. Harrick, Internal Reflection Spectroscopy, John Wiley & Sons, New York, 1967, P.30
(5) F. M. Mirbella, Jr., Appl. Spectrosc. Rev. 21 (1 & 2), 45 (1985)
(6) Seah, M. P. and Dench, W. A., Surf. Interface Anal., 1979, 1(1), 2-10
(7) Perkin Elmer, Instruction Manual for 5000 Series ESCA Systems, Version 2.0
(8) L. J. Bellamy, The Infrared Spectra of Complex Molecules, Second Edition, Chapman and Hall, 1980

Table 1: DMS Depth Profile from Angle Resolved ESCA Measurement

Solvent	Wt % DMS Bulk	Mass % DMS Not annealed		Mass % DMS Annealed	
		45°	90°	45°	90°
CH_2Cl_2	65	79.7	78.4	84.0	82.7
	50	65.3	61.9	74.2	70.0
	25	58.0	56.0	79.0	71.6
$CHCl_3$	65	78.5	76.9	81.8	79.4
	50	68.1	67.6	68.6	65.2
	25	65.5	59.1	80.6	73.3
CCl_4	65	69.0	67.7	47.7	45.6
	50	67.4	65.4	55.2	48.6
	25	insol.#	insol.	insol.	insol.
C_6H_6	65	77.1	75.1	81.7	79.0
	50	66.3	63.5	70.7	66.0
	25	47.5	43.9	64.0	58.7
C_5H_5N	65	78.4	76.5	78.3	77.2
	50	71.2	68.6	68.0	62.7
	25	52.3	47.0	63.7	58.3
C_4H_8O	65	79.0	78.2	80.3	79.5
	50	68.2	64.8	71.3	67.3
	25	55.0	49.3	73.4	65.6

Insol.: Samples are not soluable in CCl_4.

Table 2: Mass % DMS from ATR(45°)-FTIR Measurement

Solvent	Composition in Bulk (DMS/BPAC)	Mass % DMS	
		Not Ann.	Ann.*
Methylene dichloride	65/35	73.1	73.1
	50/50	51.9	51.8
	25/75	27.4	24.8
Chloroform	65/35	71.2	74.9
	50/50	53.2	50.8
	25/75	28.1	24.4
Carbon tetrachloride	65/35	72.5	70.8
	50/50	57.9	57.0
	25/75	insol.	insol.
Benzene	65/35	74.9	73.8
	50/50	52.5	59.4
	25/75	25.8	29.6
Pyridine	65/35	75.6	78.2
	50/50	56.6	55.6
	25/75	31.6	25.4
Tetrahydro-furan	65/35	73.1	74.5
	50/50	50.5	50.0
	25/75	24.9	26.1

* Ann: The sample was annealed at 180°C for 17 hours.